

A neutron scattering study of polyethylene deformed by rolling

Stephen J. Spells* and Emmanuel U. Okoroafor†

Materials Research Institute, Sheffield Hallam University, Pond Street, Sheffield S1 1WB, UK

(Received 9 November 1993)

Polyethylene mixed crystal mats have been studied after rolling at room temperature to roll ratios up to 2.5, using the LOQ instrument at the ISIS pulsed neutron source (RAL, Chilton). Radius of gyration measurements for vertical (R_V) and horizontal (R_H) sectors, where the vertical sector includes the roll direction, show that R_H is virtually unchanged by rolling, whereas R_V is increased significantly. Combined with an unchanged intensity from extrapolation to zero angle, these results indicate the absence of local melting during deformation. Intermediate angle measurements show a decrease in intensity, while the 'sheet-like' form of the scattering is retained. This is consistent with the breakup of lamellae into progressively smaller blocks, within which the original stem arrangement is preserved.

(Keywords: neutron scattering; mixed crystal; polyethylene)

INTRODUCTION

Neutron scattering techniques are increasingly being used to study oriented polymers and the processes of orientation, largely because of the details of molecular conformation obtainable. In the case of polyethylene, the range of materials to be studied includes high modulus polymer from solid state extrusion and from pressure-induced crystallization during capillary flow¹, melt crystallized polymer after shear deformation² and after drawing through a neck^{3,4} and single crystal mats drawn through a neck⁵. Apart from the details of chain trajectory, obtainable through the radius of gyration and the form of the scattering curve in intermediate and wide-angle neutron scattering (IANS and WANS, respectively), determination of the onset of isotopic fractionation has proved a useful indication of local melting and recrystallization^{3,5}.

Mixed crystal i.r. spectroscopy is another well established experimental method for the study of molecular conformation in polyethylene, and the two techniques in combination have been shown to allow detailed and relatively unambiguous information on the path taken through the lamellar crystal by a molecule. Solution grown crystals⁶⁻⁸ and annealed crystals^{9,10} have previously been studied by these techniques. In the accompanying paper¹¹, mixed crystal i.r. spectroscopy, together with other methods of characterization, has been applied to single crystal mats deformed by rolling at room temperature. It was shown that the original lamellae break up progressively with increasing roll ratio ϵ , with rotation and translation of the separating blocks. The molecular (c) axis moves towards the roll direction, with

the b -axis remaining within the mat plane. Under these conditions of rolling, there is no evidence of refolding, although the crystallite stacking regularity is greatly disrupted. A co-ordinated study of chain conformational changes on rolling has been undertaken, using a range of appropriate techniques, and the present work involves the neutron scattering part of this study. While the i.r. technique allows direct analysis of the breakup of groups of labelled stems on deformation, hence enabling the reduction in block size to be followed, neutron scattering is dependent on the entire spatial distribution of labelled stems. For example, the radius of gyration, as determined from small-angle neutron scattering (SANS) measurements, is dependent on the overall molecular dimensions. In combination with the crystallite block sizes determined from i.r. data, SANS measurements in principle allow the separation between blocks to be determined. Once again, the neutron scattering and i.r. methods are seen to provide complementary information in determining chain conformation.

EXPERIMENTAL

Mixed crystals of normal polyethylene (PEH) and fully deuterated polyethylene (PED) were grown from dilute solution (0.05% w/v) in xylene at 70°C. PED fractions C (molecular weight $M = 63\,000$) and A ($M = 150\,000$) were used at 3% concentration, in a matrix of PEH ($\bar{M}_w = 86\,000$, $\bar{M}_n = 24\,000$). As explained in the accompanying paper¹¹, the filtered and dried mats were pressed at room temperature in order to minimize void scattering and were deformed by rolling at room temperature. For these neutron scattering measurements, a maximum ϵ of 2.5 was used.

The LOQ small-angle scattering instrument at the ISIS pulsed neutron source (RAL, Chilton) was used, with

* To whom correspondence should be addressed

† Current address: Department of Chemistry and Physics, Nottingham Trent University, Nottingham NG11 8NS, UK

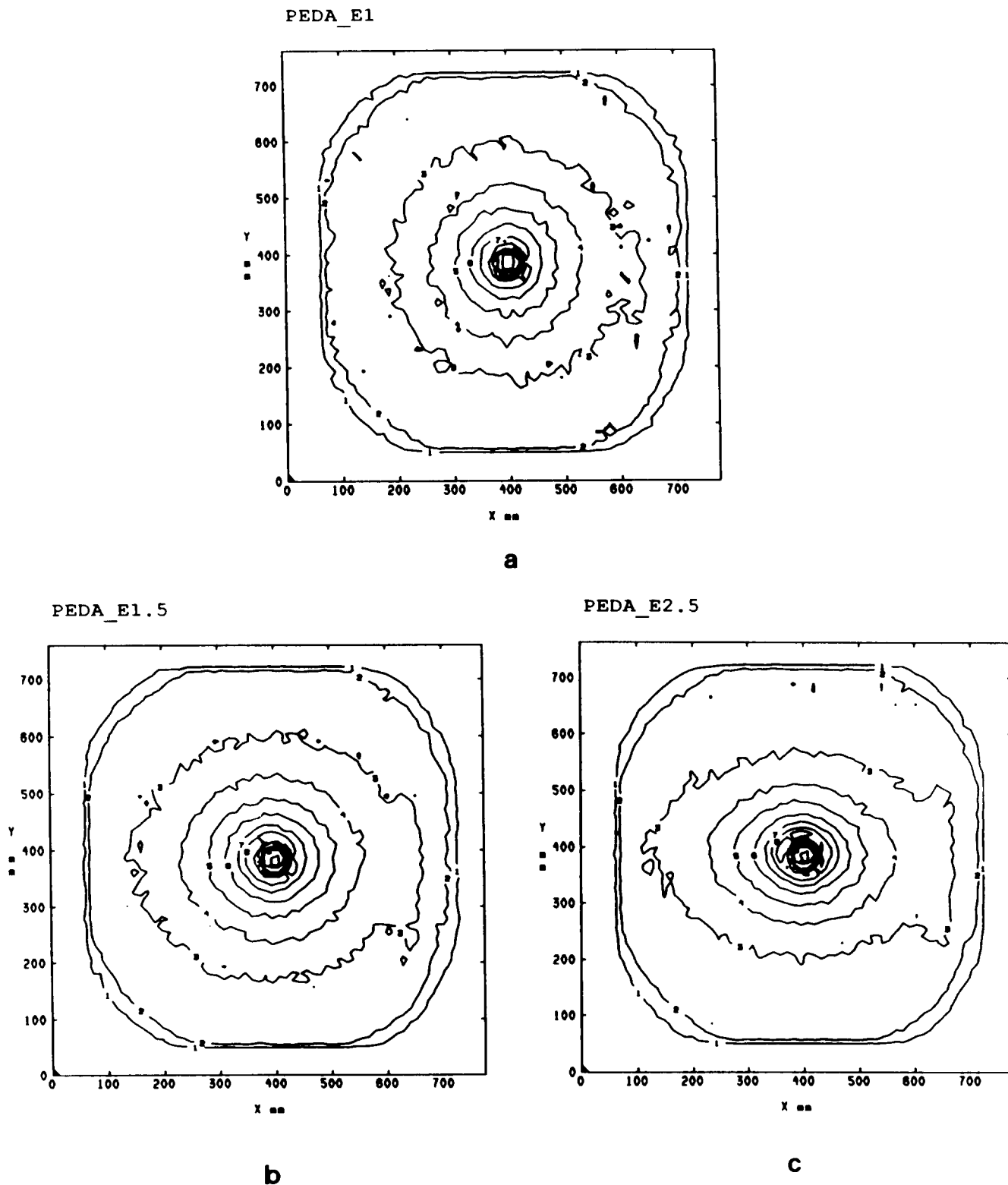


Figure 1 Contour plots of scattered neutron intensity from a sample containing 3% of PED fraction A: (a) before rolling; (b) after rolling to $\epsilon=1.5$; and (c) after rolling to $\epsilon=2.5$. In each case, there is an anomalous signal ('fish tail') to the right side of the detector

neutrons of wavelength in the range 2.2–10.0 Å and the standard detector configuration (sample–detector distance = 4.4 m). Samples with dimensions of 10 × 10 mm were stacked in the apertures of aluminium plates which were held within cadmium sample holders. A scintillation detector measuring the incident flux allowed normalization of scattering intensities. Data processing as a

function of time of flight and scattering angle made use of the Colette program. Scattering data were obtained for both deformed and undeformed samples and also for pure PEH and PED. These blank samples were not deformed, a factor which has implications for the analysis later. Allowance was also made for variation in cell response across the detector.

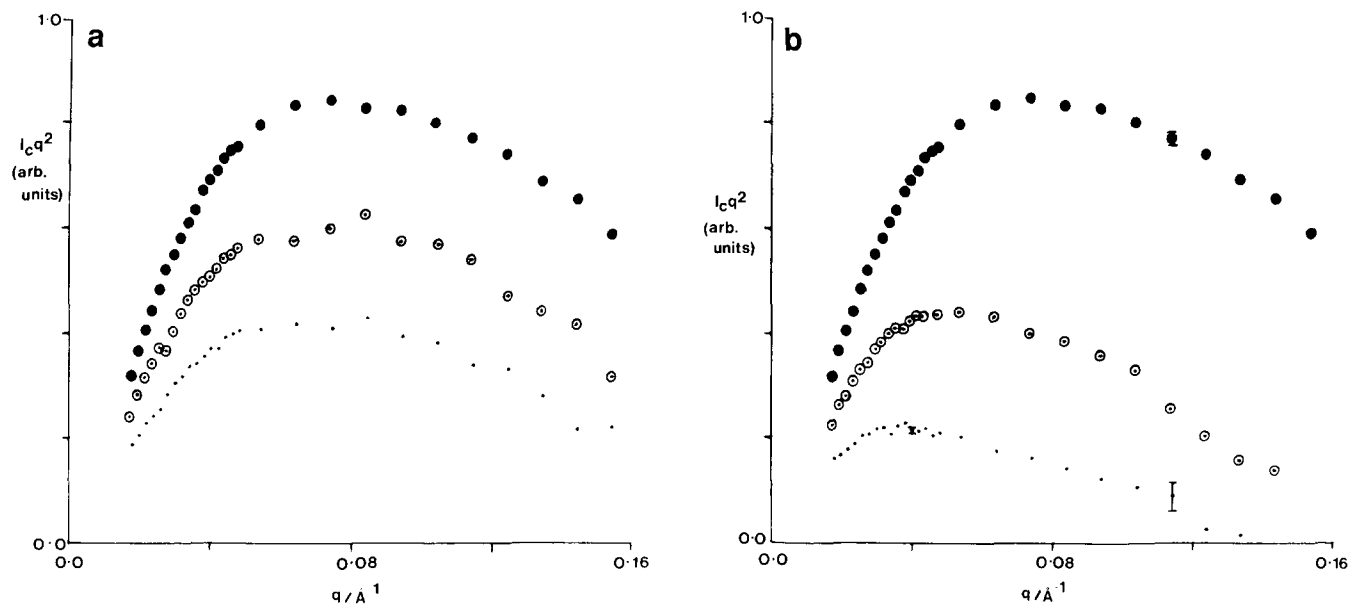


Figure 2 Kratky plots for a sample containing 3% of PED fraction A: (●) before rolling; (○) after rolling to $\varepsilon=1.5$; (◐) after rolling to $\varepsilon=2.5$. (a) Data for the sector including the horizontal direction; (b) corresponding data for the vertical (roll) direction. Representative error bars are shown

Table 1 Variation of radius of gyration with roll ratio^a

Roll ratio	Sample C		Sample A	
	R_H (Å)	R_V (Å)	R_H (Å)	R_V (Å)
1.0	71 ± 2	71 ± 2	64 ± 1	64 ± 1
1.5	66 ± 3	78 ± 2	68 ± 3	84 ± 2
2.5	88 ± 5	115 ± 3	69 ± 2	125 ± 14

^a R_H and R_V refer to radii of gyration for sectors including the horizontal and vertical directions, respectively, for samples containing 3% of the PED fractions indicated

RESULTS

Figure 1 shows typical intensity contour plots obtained from the BF_3 -filled multiwire detector. Despite the anomalous 'fish tail' intensity distribution to the right of the detector, the data clearly show the development of molecular anisotropy with increasing ε . The Colette program allows the analysis of such anisotropic data, using sectors of predetermined angular width. A width of 30° was chosen as a suitable compromise between angular resolution and signal to noise ratio. The vertical sector in each case included the roll direction. Zimm plots were obtained in the region $q \leq 0.044 \text{ \AA}^{-1}$, and the results are shown in Table 1. The vertical radius of gyration (R_V) increases significantly on rolling, while the horizontal radius (R_H) generally shows no significant change. In the case of sample A rolled to $\varepsilon=2.5$, the Zimm plot for the vertical sector showed some curvature, and the angular range for fitting was reduced to $q \leq 0.034 \text{ \AA}^{-1}$. Nevertheless, the result shows a larger error in gradient than other data. When considering the lamellar crystalline nature of the mats, the deformation is not expected to be affine.

The fact that R_H remains virtually unchanged up to $\varepsilon=2.5$ leads to two conclusions. First, isotopic fractionation, which would lead to a redistribution of labelled stems and hence modify both R_H and the i.r. spectrum, does not occur. The intercept $1/I_0$ (where I_0 is the zero angle scattering intensity) extrapolated from Zimm plots also shows insignificant change on rolling, confirming

this view. Therefore, there is no local melting under the deformation conditions used here. Second, the labelled stem distribution perpendicular to the roll direction is largely unaffected by rolling.

IANS data are shown in Figure 2 for both vertical and horizontal sectors. The data are shown in the form of Kratky plots, where the experimental intensities, $I(q)$, have been modified to give equivalent intensities for infinitely thin stems, $I_c(q)$, using:

$$I_c(q) = \frac{I(q)}{C(q)} \quad (1)$$

Here $C(q)$ is the ratio of the intensity from a real stem to that from a thin stem. This format allows immediate comparisons with simple model situations, such as that of randomly arranged stems⁶. As expected from the different sample molecular weights⁶, the two samples show different scattering curves before rolling. Deformation produces a decrease in scattered intensity, with appreciable changes in the case of the vertical sector. However, the characteristic 'sheet-like' angular dependence of scattering, with an approximately linear variation of Iq^2 beyond the peak in this function, is largely preserved within this angular range. A similar observation was made for single crystal mats annealed without deformation⁹. In the present case, besides the modifications to labelled stem positions there is also the effect of changes in crystallite orientation. It has been shown⁶ that destruction of the c -axis orientation of single crystal mats to produce an isotropic sample yields scattered intensities of about half of the former values, without changing their angular dependence significantly. It may, therefore, be deduced that changes in angular dependence of the IANS data result primarily from changes in labelled stem positions. A further complication in the present data analysis arises from the fact that undeformed blank (pure PEH and PED) samples were used here: production of rolled PED samples of suitable thickness presents particular problems. From the unusually low scattering intensities obtained at the widest angles ($q \approx 0.21 \text{ \AA}^{-1}$), it appears that this introduces significant subtraction

errors. We therefore confine our attention to the angular range of Figure 2, and treat model calculations with some caution. For the same reason, an absolute intensity scale is not given in the figures. Nevertheless, the results are consistent with those from i.r. analysis¹¹, showing that the groups of labelled stems are progressively broken up on deformation, but that some larger groups, characterized by stems still arranged on several sheets, are retained.

MODEL CALCULATIONS

Models of crystallite breakup, involving the detailed analysis of the changes in size of groups of labelled stems during deformation, have proved particularly useful in interpreting i.r. data¹¹. The effects on the i.r. spectrum of specific crystallographic crack directions have been evaluated and compared with experimental results. For the reasons outlined above, a similarly detailed analysis of neutron scattering data is not feasible. However, it is useful to demonstrate the trends expected in IANS data with increasing ϵ , and for this reason calculations have been carried out using similar molecular models to those used for the i.r. analysis.

To model the full molecular conformation, we require not only the sizes of crystal blocks which break away from the original lamellae (as in the i.r. case) but also the distances by which the blocks become separated. Since the value of R_v depends on both the block size and the crack size, knowledge of the former from i.r. results¹¹ should allow the crack size to be determined by use of neutron data. However, a complication arises in that a uniform block size (as in the i.r. analysis) together with a uniform crack dimension, as may be suggested here for the sake of simplicity, would lead to preferred periodicities in labelled stem separations. Such a situation, although attractive in its simplicity, is clearly not physically realistic. A Gaussian distribution of crack sizes was therefore considered. This has the disadvantage of introducing additional model parameters, and inevitably leads to some uncertainty in the average values of crack dimensions required to fit experimental data. In each case, the radius of gyration was calculated for each molecular configuration generated, and the results were averaged both before and after 'deformation' to enable comparison with experimental results.

As in the accompanying¹¹ and previous^{8,9} work, we take as our starting point the molecular model for as-grown single crystals of polyethylene incorporating sheets of labelled crystal stems linked by 'superfolds'. The model involves a dilution of crystal stems along the fold plane from one molecule by stems from other molecules to the extent of 50%, with 75% of folds connecting adjacent stems and a molecular weight per sheet of 21 000. Starting molecular configurations were generated using these statistical parameters for each crystallographic crack direction to be considered. Each configuration was then divided into blocks of equal size (as determined from i.r. measurements¹¹), with a block separation distance chosen to be consistent with the observed ratio of R_v values for rolled and unrolled samples.

As discussed in earlier work on solution-grown single crystals^{6,9}, the calculation can be simplified by recognizing: (1) that most monomer units are within crystal stems; and (2) that the c -axis orientation within single crystal mats reduces the problem of specifying stem arrangements to a two-dimensional one (although this

situation is clearly changed on rolling). The scattered intensity $I_c(q)$, from an array of structureless stems can be expressed as:

$$I_c(q) = \frac{n_L \pi}{q} \int \Gamma(R) J_0(qR) dR \quad (2)$$

where n_L is the number of labelled atoms per unit length of crystal stem and $\Gamma(R)$ is the spatial correlation function for stems with a separation of R . A Monte-Carlo method⁶ can be used to sample the stem positions generated, and hence obtain $\Gamma(R)$.

Because of uncertainties, described earlier, in the true distribution of crack dimensions in the rolled samples, we do not include here the full results of model calculations of scattered intensity, but concentrate instead on the radius of gyration calculations and 'representative' crack dimensions, listed in Table 2. In summary, IANS calculations for a particular block size show little dependence on the crack direction, considering cracks in the a -, b - or non-folding $\langle 110 \rangle$ directions. It is, therefore, not possible to state whether or not these mechanisms operate together, during deformation. It is noticeable from Table 2 that the observed radii of gyration for undeformed mats are somewhat larger than calculated values, as has been noted previously¹²; small changes in the extent of 'overlap' of neighbouring sheets give rise to large changes in the calculated values. Nevertheless, the calculated ratios of the radii of gyration in the roll direction for deformed and undeformed mats agree well with those determined experimentally. The crack sizes quoted here should be considered only as rough estimates.

CONCLUSIONS

Neutron scattering methods provide useful structural information to complement the findings from our i.r. study¹¹. SANS data show that the radius of gyration in the roll direction of the mats increases, while in the perpendicular direction there is no significant change. This latter feature, along with the absence of any change in the extrapolated zero angle intensity, indicates that local melting does not occur. While the i.r. technique has enabled the size of blocks breaking from the original lamellae to be determined, values obtained for the radius of gyration additionally allow the block separations to be estimated. At $\epsilon = 2.5$, the block size is determined to be 85 Å, while the block separation increases to ~ 24 Å.

IANS data provide confirmation that the sheet-like structure of single crystals is preserved, at least up to $\epsilon = 2.5$. The results support the evidence from i.r. measurements that there is a progressive breakup of crystallites into smaller blocks, with some larger groups of labelled stems preserved at these levels of deformation. As with i.r. spectroscopy, it is not possible to choose between

Table 2 Calculated dimensions of structural units

Roll ratio	Crystallite block size (Å) ^a	Crack size (Å) ^b	Calculated R_v (Å) ^c	
			Sample C	Sample A
1.0	—	—	53	59
1.5	107	10	68	77
2.5	85	24	80	95

^a Dimensions calculated from i.r. data¹¹

^b Estimates on the basis of this work

^c From model calculations in this work

three crystallographic directions for the direction of cracks, and it is likely that these processes take place in combination.

ACKNOWLEDGEMENTS

We are grateful to the SERC for support for one of us (EUO). We would like to thank Dr R. K. Heenan (RAL, Chilton) for assistance with neutron scattering measurements and Mrs A. Halter (University of Bristol) for providing PED fractions.

REFERENCES

- 1 Sadler, D. M. and Odell, J. A. *Polymer* 1980, **21**, 479
- 2 Wu, W., Wignall, G. D. and Mandelkern, L. *Polymer* 1992, **33**, 4137
- 3 Sadler, D. M. and Barham, P. J. *Polymer* 1990, **31**, 36
- 4 Sadler, D. M. and Barham, P. J. *Polymer* 1990, **31**, 46
- 5 Sadler, D. M. and Barham, P. J. *Polymer* 1990, **31**, 43
- 6 Spells, S. J. and Sadler, D. M. *Polymer* 1984, **25**, 739
- 7 Spells, S. J., Keller, A. and Sadler, D. M. *Polymer* 1984, **25**, 749
- 8 Spells, S. J. *Polymer* 1985, **26**, 1921
- 9 Sadler, D. M. and Spells, S. J. *Macromolecules* 1989, **22**, 3941
- 10 Spells, S. J. and Sadler, D. M. *Macromolecules* 1989, **22**, 3948
- 11 Okoroafor, E. U. and Spells, S. J. *Polymer* 1994, **35**, 4578
- 12 Sadler, D. M. and Keller, A. *Science* 1979, **203**, 263